Calcium oscillation linked to pacemaking of interstitial cells of Cajal; Requirement of calcium influx and localisation of TRP4 in caveolae

(With 8 figures)

By

Shigeko Torihashi, Toyoshi Fujimoto,

Claudia Trost¶ & Shinsuke Nakayama*

From

Department of Anatomy and Cell Biology, and *Department of Cell Physiology,

Nagoya University Graduate School of Medicine,, Nagoya 466-8550, JAPAN

¶Institute für Pharmakologie und Toxikologie, Universität des Saarlandes, D-66421

Homburg, Germany

***Short title* :** Calcium oscillation in interstitial cells of Cajal

***Author for Correspondence*:** Shigeko Torihashi,

Department of Anatomy and Cell Biology, Nagoya University Graduate School of Medicine, 65 Tsurumai, Showa-ku, Nagoya 466-8550, JAPAN.

Direct line: +81 52 744 2001 FAX: +81 52 744 2012

e-Mail: storiha@med.nagoya-u.ac.jp

Summary

Interstitial cells of Cajal (ICC) are considered to be pacemaker cells in gastrointestinal tracts. ICC generate rhythmical electronic activity as slow waves, which is dihydropyridine- insensitive, and drive spontaneous contraction of smooth muscles. Although cytosolic Ca^{2+} has been assumed to play a key role in pacemaking, Ca^{2+} movements in ICC have not yet been examined in detail. In the present study, using cultured cell clusters isolated from the mouse small intestine, we demonstrated Ca^{2+} oscillations in ICC. Fluo4 was loaded to the cell cluster, the relative amount of cytosolic Ca^{2+} was recorded, and ICC were identified by c-Kit immunoreactivity. We specifically detected Ca^{2+} oscillation in ICC in the presence of dihydropyridine, which abolishes Ca^{2+} oscillation in smooth muscles. The oscillation was coupled to the electrical activity corresponding to slow waves and depended on Ca^{2+} influx through a non-selective cation channel, which was SK&F 96365-sensitive and store-operated. We further demonstrated the presence of transient receptor potential-like channel 4 (TRP4) in caveolae of ICC. Taken together, the results infer that the Ca^{2+} oscillation in ICC is intimately linked to the pacemaker function and depends on Ca^{2+} influx mediated by TRP4.

Introduction

Interstitial cells of Cajal (ICC) are a distinct and unique cell population distributed in the gastrointestinal (GI) muscle layer of many vertebrates including humans (1-2). They are network-forming cells connected electrically with each other and with smooth muscle cells via gap junctions. GI muscle shows spontaneous rhythmical contractions accompanied by periodic electrical oscillation, i.e., so-called slow waves which are affected by neither tetrodotoxin (TTX; blocker of nervous activity) nor dihydropyridine (blocker of L-type calcium channel) (3-5). It has been postulated that ICC are pacemaker cells that generate slow waves and induce spontaneous contractions of the smooth muscles.

In the last decade, ICC were found to express the proto-oncogene *c-kit* and to develop depending upon activation of *c-kit* signal pathways (4, 6-8). The expressions of *c-kit* and/or c-Kit receptors have been commonly used as a marker of ICC in the GI muscle layers and also enables the isolation of ICC. Recent electrophysiological studies using isolated ICC have demonstrated periodic oscillations of the membrane current (9-11). Thus, ICC have been considered as pacemaker cells in recent years.

The intrinsic properties underlying the pacemaking mechanism in ICC have been emphasised in previous reports (11). Several groups have reported that generation of electrical rhythmicity involves Ca^{2+} release through inositol trisphosphate (IP3) type 1 receptor in the endoplasmic reticulum (ER) and subsequent Ca^{2+} entry into mitochondria (12-14). From these results, periodic rises in the cytosolic (intracellular) Ca^{2+} concentration ($[Ca^{2+}]_i$) are considered to play a key role in generating slow waves. However, such $[Ca^{2+}]_i$ oscillation has not yet been analysed precisely. Currently, using Ca^{2+} imaging techniques, Yamazawa and Iino have demonstrated Ca^{2+} transients in ICC and longitudinal smooth muscles (15). Their results suggested that $[Ca^{2+}]_i$ played a crucial role in pacemaking and that Ca^{2+} imaging at the tissue level was a useful technique to investigate slow wave propagation in GI muscle. It is, however, necessary to clearly identify the distribution of ICC and their $[Ca^{2+}]_i$ in order to analyse the mechanism

underlying the generation of electrical rhythmicity in ICC. In the present study we recorded fluorescent Ca^{2+} images where ICC were identified by c-Kit immunostaining in small cell clusters isolated from GI muscle. The observed $[Ca^{2+}]_i$ oscillation was sensitive to neither TTX nor dihydropyridine so that it was isolated from $[Ca^{2+}]_i$ in smooth muscles in the presence of nifedipine.

In contrast to the intracellular Ca^{2+} circuit, periodic activation of plasmalemmal channels to generate pacemaker current has not been demonstrated, though several candidates such as non-selective cation channels including TRPs, Cl^- channels, and/or Ca^{2+} activated K^+ channels have been reported (5, 8, 16-18). To address this, we investigated the pharmacological properties of $[Ca^{2+}]_i$ oscillation and the influx in ICC using cultured cell clusters. We also examined expression of putative channels by immunohistochemistry. Our result indicates that $[Ca^{2+}]_i$ oscillation in ICC requires a Ca^{2+} influx and TRP4 is at best a candidate for the mediator.

A preliminary description of the results was provided at the 18th International Symposium on Gastrointestinal Motility (November 15-19, 2001; Madison, WI, USA) (19).

Experimental Procedures

Preparation of cultured cell clusters

BALB/c mice (10-15 days after birth) of either sex were used. Animals were treated according to the *Guide to Animal Use and Care of the Nagoya University School of Medicine*. Smooth muscle layers of small intestines were separated from the mucosa and cut into small pieces, and then incubated in Ca^{2+}-free Hanks' solution containing collagenase (1.3 mg/ml, Wako Chemical), trypsin inhibitors (2 mg/ml), ATP (0.27 mg/ml) and bovine serum albumin (2 mg/ml) for 40-45 min at 37°C. After rinsing with an enzyme-free solution (without collagenase and trypsin inhibitors), the muscle pieces were triturated with fire-blunted glass pipettes. The resultant small cell clusters were placed onto murine collagen-coated coverslips in 35-mm culture dishes, and were incubated in a culture medium (DMEM) supplemented with 10% foetal bovine serum, streptomycin (100 U/ml) and penicillin (100 μg/ml) at 37 °C. After 2-4 days of incubation, the cultured cell clusters were used for Ca^{2+} imaging.

Ca^{2+} imaging

The cultured cell clusters were incubated for two hours (at room temperature) in a modified Krebs solution containing 10 μM fluo4 acetoxymethyl ester (Dojindo) and detergents (0.02 % Pluronic F-127, Dojindo or 0.02 % cremophor EL, Sigma). A CCD camera system (Argus HiSCA, Hamamatsu Photonics) combined with an inverted microscope was used to monitor oscillation of the intracellular Ca^{2+} concentration ($[Ca^{2+}]_i$). $[Ca^{2+}]_i$ in ICC was measured in the presence of 1 μM nifedipine (Sigma). The cell clusters were illuminated at 488 nm, and fluorescent emissions of 515-565 nm were recorded at an intensity of fluo4. Digital Ca^{2+} images (328 x 247 pixels) were normally collected at 100-400 ms intervals. Because fluo4 is a single wavelength indicator, it was not possible to apply the ratiometric method for quantitative determination of $[Ca^{2+}]_i$. Therefore, the intensity of fluo4 fluorescence was normalised in the temporal analysis. The temporal fluorescent intensity of the dyes (Ft) was divided by the fluorescence

intensity at the start (F0). These relative values represent integrated $[Ca^{2+}]_i$. After recording of the fluorescent intensity with nifedipine, localisation of ICC were examined by c-Kit immunohistochemistry and small c-Kit-positive points (2μm in diameter) were analysed as $[Ca^{2+}]_i$ in ICC. c-Kit-negative points of the same size were recorded as non-ICC regions. During Ca^{2+} imaging, the temperature of the recording chamber was kept at 35 °C using a modified micro-warm plate system (DC-MP10DM, Kitazato Supply), and the bath solution was circulated at 0.5 ml / sec.

Simultaneous recording of electrical activity and $[Ca^{2+}]_i$.

In some cell clusters, electrical activity was also measured using a differential amplifier (DP-301, Warner Instrument Corp. USA) and a recticorder (RJG-4022, Nihon Koden, Japan). The amplifier was operated in an AC mode (high pass = 0.1 Hz; gain = 1,000). A cut-off frequency of 100 Hz was applied to reduce the noise. Glass pipettes with tips smaller than 10 μm in diameter were filled with modified Krebs solution written bellow, and put on the middle of cell clusters during Ca^{2+} imaging.

Immunohistochemistry and western blotting

The cell clusters used for Ca^{2+} imaging were treated for 5 min with rat anti-c-Kit antibody (ACK2, 10 μg/ml; (7)) conjugated with Alexa Fluoro 594 (Molecular probes). After washing with modified Krebs solution, they were fixed with ice cold acetone for 2 min and observed by a confocal laser microscope (LSM5 PASCAL, Zeiss Germany). These samples were incubated with mouse anti-γ-enteric actin antibody (1:200; ICN) again and subsequently treated with goat anti-mouse IgG conjugated with FITC (1:200; Vector), followed by re-examination of the same clusters by confocal microscopy. Instead of the procedure described above, some cell clusters were fixed with 4% paraformaldehyde in 0.1 M phosphate buffer (pH 7.4 at 4°C) for 30 min. They were then incubated with rabbit anti-PGP9.5 antibody (1:8000; UltraClone) and treated with goat anti-rabbit IgG conjugated with Texas Red (1:200; Vector) for confocal microscopy. To examine TRP4 immunoreactivity on ICC, muscle layers fixed with ice cold acetone for 5

min were treated as whole mount preparations for double labelling with rabbit anti-TRP4 antibody (1:100, either from Alomon Labs corresponding to residues 943-958 of mouse TRP4, or Ab236 corresponding to residue 969-981 of bovine TRP4 (20)) and ACK2. They were detected by goat anti-rabbit IgG with FITC and goat anti-rat IgG with Texas Red (Vector). Rabbit anti-TRP6 antibody (1:100, Alomon Labs corresponding residues 24-38 of mouse TRP6) was also used in the same manner. Another double staining with anti-TRP4 and mouse anti-caveolin 1 antibodies (1:20, Transduction Lab., Lexington, KY) was tried to cultured cell clusters after Ca^{2+} imaging and demonstrated by goat anti-rabbit IgG with Texas Red and goat anti-mouse IgG with FITC, respectively. The specificity of immunoreactivity was checked by controls in which primary antibodies were omitted from the initial incubation. For an examination of the expression of TRP4 and TRP6 in the muscle layer, western blotting was carried out. The muscle layer was homogenised, separated by SDS-PAGE, blotted onto nitrocellulose membrane and probed by anti-TRP4 and anti-TRP6 antibodies. Antibodies pre-incubated with excess antigens were also used to check the specificity and applied to both immunohistochemistry and western blotting. The membranes were further incubated with HRP-conjugated goat anti-rabbit IgG (Amersham), and reactions were visualised by Supersignal West Dura Extended Duration Substrate (Pierce).

Immunoelectron microscopy

Muscle layers were fixed with 2% paraformaldehyde in 0.1 M phosphate buffer, pH 7.4, and cut into small pieces. After fixation for 30 min at 4°C, samples were infused with a mixture of sucrose and polyvinylpyrrolidone (Sigma; (21)), and frozen rapidly in liquid nitrogen. Ultrathin cryo-sections (50-70 nm) were incubated with rabbit anti-TRP4 antibody (1:100, Ab236), and processed for indirect immunostaining with 5 nm colloidal gold-conjugated goat anti-rabbit IgG (Amersham). The sections were embedded in a mixture of 2% methylcellulose (Nacalai) and 0.5% uranyl acetate (22). They were then examined by an electron microscope (H-7000, Hitachi).

Solutions

The modified Krebs solution was used as a normal solution in Ca^{2+} measurements, and had the following composition (mM): NaCl, 125; KCl, 5.9; $CaCl_2$, 2.5; $MgCl_2$, 1.2; glucose, 11.8 and Hepes, 11.8; pH was adjusted to 7.4-7.5 with Tris base. For a Ca^{2+} -free solution, $CaCl_2$ was replaced with NaCl. Several salts such as $MnCl_2$, $NiCl_2$, $LaCl_3$ and $CdCl_2$ were added to the bath solution. SK&F 96365 and thapsigargin were purchased from Biomol Research Laboratories, Inc.

Statistics

Numerical data are expressed as mean ± standard deviation.

Results

Structure of cell clusters and c-Kit immunopositive cells

Small pieces of tissue developed into round or ovoid clusters after 2-4 days in culture, and were attached to the coverslips. The clusters were mainly composed of smooth muscle cells positively stained with anti-γ-enteric actin antibody (Fig. 1A, B), and most of them included c-Kit-positive ICC. The distribution pattern of ICC, however, was disturbed (Fig. 1C). In large cell clusters (more than 100 μm in diameter), enteric neurons were also included (Fig. 1D).

Calcium oscillation in cultured cell clusters

Under superfusion with a modified Krebs solution at 35°C, the cultured cell clusters showed periodic contractions at a rate of 19 ± 3.8 cycles / min (n = 27). The contractions were always associated with periodic depolarization in the cell membrane, i.e., slow waves (measured using patch clamp techniques; unpublished observation of Nakayama and Torihashi). Emission light of fluo4 in these clusters was monitored using a CCD camera system. Figure 2 shows an example of such experiments, and the movement of $[Ca^{2+}]_i$ is indicated by pseudocolour ratioed images (Fig. 2A, B). Although the amount of fluorescent dye loaded to each cell varied, many cells clearly showed a

synchronised $[Ca^{2+}]_i$ oscillation, followed by contractions of the cluster. In Figure 2C, changes in the fluorescent intensity were measured at the three points indicated in Figure 2A and 2B. $[Ca^{2+}]_i$ oscillation was also monitored in the presence of 250 nM TTX, which should completely suppress nerve activities. Neither periodic changes in the $[Ca^{2+}]_i$ concentration nor contractility were affected by this treatment (data not shown).

Dihydropyridine derivatives (nifedipine), which selectively block voltage-sensitive L-type Ca^{2+} channels and consequently prevent smooth muscle contraction, are known to scarcely affect slow waves in the mouse small intestine. In the presence of nifedipine, we further examined properties of $[Ca^{2+}]_i$ oscillation in cultured cell clusters. There were regional dihydropyridine-resistant $[Ca^{2+}]_i$ oscillations in the cluster, though the contractile activity of the cluster was suppressed (Fig. 3A-C). Points (1) and (2) in Figure 3A and 3B indicate regions inside a cluster showing such $[Ca^{2+}]_i$ oscillation during exposure to 1 μM nifedipine. On the other hand, point (3) in Figure 3A and 3B did not show such movement. The maximum and minimum levels of $[Ca^{2+}]_i$ indicated by pseudocolour ratioed images during $[Ca^{2+}]_i$ oscillation are shown in Figures 3A and 3B. The time course analysis of $[Ca^{2+}]_i$ oscillation is presented in Figure 3E (dihydropyridine-resistant oscillations at points (1), (2) and at dihydropyridine-sensitive point (3)). The frequency of dihydropyridine-resistant $[Ca^{2+}]_i$ oscillation was 21 ± 4.1 cycles/min (n=30), and similar to that seen in the solution without nifedipine described above. The phase-contrast microscopy (Fig. 3C) and the c-Kit immunohistochemistry (Fig. 3D) obtained from the same cell cluster used in Figures 3A-D indicate localisation of c-Kit positive cells in the cluster. Points (1) to (3) in Figure 3D respectively correspond to those indicated in Figure 3A and 3B. Comparison of Figure 3A and 3B with 3D clearly demonstrated that points (1) and (2) corresponded to c-Kit immunopositive regions and generated $[Ca^{2+}]_i$ oscillation. On the other hand, point (3) originated from a c-Kit negative region and did not show $[Ca^{2+}]_i$ oscillation. We obtained similar results in thirty out of 35 cell clusters examined. This indicates that ICC identified by c-Kit immunostaining show dihydropyridine-resistant $[Ca^{2+}]_i$ oscillation, and that

they play an important role in generating spontaneous rhythmicity in the cluster.

$[Ca^{2+}]_i$ oscillation in ICC and electrical activity

Electrical activity corresponding to slow waves was measured using an extra-cellular recording technique. Simultaneous recordings of the electrical activity and $[Ca^{2+}]_i$ oscillations in ICC with 1 μM nifedipine are shown in Figure 4. The frequency of both slow waves and $[Ca^{2+}]_i$ oscillation in ICC (thick line) was scarcely affected by nifedipine, although $[Ca^{2+}]_i$ in a c-Kit negative region (thin line) did not show oscillation. We obtained same results in four out of 5 cell clusters. The frequency of slow waves and $[Ca^{2+}]_i$ oscillation in ICC were the same, and their movements coincided with each other, reflecting a close temporal relationship. The frequency was 17 ± 3.3 cycle/ min (n = 4), and the amplitude of the electrical activity averaged 0.25 ± 0.02 mV (n = 4).

Characteristic properties of $[Ca^{2+}]_i$ oscillation in ICC

When Ca^{2+} free solution was applied in the presence of 1 μM nifedipine, the amplitude of $[Ca^{2+}]_i$ oscillation in ICC decreased and subsequently disappeared (n = 5; Fig. 5A). Modified manganese quenching (200 μM of $MnCl_2$ and 1 μM of nifedipine in a Ca^{2+} free bath solution) also abolished $[Ca^{2+}]_i$ oscillation in ICC (n = 4; Fig. 5B). These results indicate that $[Ca^{2+}]_i$ oscillation in ICC required extracellular Ca^{2+}. Since nifedipine does not block $[Ca^{2+}]_i$ oscillation in ICC, the L-type Ca^{2+} channel is not likely to be involved in the Ca^{2+} influx of ICC. We then examined the effects of several cations with 1 μM nifedipine. La^{3+} (50 μM) markedly reduced the amplitude of $[Ca^{2+}]_i$ in the cluster and blocked $[Ca^{2+}]_i$ oscillation in ICC (n = 7; Fig. 5C). Cd^{2+} (100 μM) increased the intensity of fluo4 fluorescence in the cluster and disturbed $[Ca^{2+}]_i$ oscillation in ICC (n = 6; Fig. 5D). On the other hand, Ni^{2+} (50 μM), known to be a blocker of T-type calcium channel, did not affect $[Ca^{2+}]_i$ oscillation rhythms in ICC (n = 5; Fig. 5E). When a small amount of SK&F 96365 (4 μM), which blocks TRP, was added to the bath solution with nifedipine, it significantly reduced the amplitude and prevented $[Ca^{2+}]_i$ oscillation in ICC (n = 5; Fig. 6A). Some TRP have been suggested to be involved in Ca^{2+} entry mediated

by store depletion (SOCs). When a Ca^{2+} pump blocker, thapsigargin, was added at 5 μM, the Ca^{2+} level rose once and then subsided along with a diminution of $[Ca^{2+}]_i$ oscillation in ICC (n = 4; Fig. 6B). Thapsigargin combined with nifedipine in the Ca^{2+} free solution quickly blocked $[Ca^{2+}]_i$ oscillation in ICC. However, no transient increase in the Ca^{2+} level was recorded (n = 3; data not shown).

Immunohistochemistry and cytochemistry for TRP proteins

Expressions of TRP proteins were investigated by immunohistochemistry on a whole mount preparation of the smooth muscle layer. Double staining with anti-c-Kit and anti-TRP4 antibodies revealed the TRP4 immunoreactivity in c-Kit immunopositive ICC at the myenteric plexus level (Fig. 7A-D). Not only ICC but also other supposedly smooth muscle cells expressed TRP4. The TRP4 expression in ICC was stronger than in the putative smooth muscle cells (Fig. 7B). The two antibodies used for TRP4 immunohistochemistry showed similar results. Although TRP6 was also positive in the smooth muscle layer as confirmed by western blotting (Fig. 7E), double immuno-staining for TRP6 and c-Kit did not detect TRP6 in ICC (data not shown). The fine localisation of TRP4 in ICC was studied using cell clusters by double labelling immunohistochemistry for TRP4 and caveolin-1in ICC where $[Ca^{2+}]_i$ oscillation was recorded in the presence of nifedipine. This double staining demonstrated that localisation of TRP4 largely coincided with caveolin-1 (n = 10; Fig. 8A-D). Immunoelectron microscopy further confirmed that TRP4 was mostly distributed in caveolae in ICC, which were located between the circular and longitudinal muscle layer and identified as ICC morphologically (n = 5; Fig. 9).

Discussion

In the present study, we observed slow periodic contractions accompanied by $[Ca^{2+}]_i$ oscillations in cell clusters after 2-4 day culture. Immunohistochemistry revealed that smooth muscle cells, c-kit positive ICC and sometimes enteric neurons were included in these clusters (Fig. 1). A blockade of the nervous activities with TTX, however, affected neither contractility nor $[Ca^{2+}]_i$ oscillation, suggesting that enteric neurons were not indispensable for the generation of the basic spontaneous activity. We assume that the neurons might modulate the basic rhythmicity and co-ordinate the activity of neighbouring contractile units (23). It is also well known that dihydropyridine (nifedipine) blocks L-type Ca^{2+} channels in smooth muscle cells and inhibits their contractions. Our Ca^{2+} imaging in the presence of nifedipine, therefore, excludes $[Ca^{2+}]_i$ oscillation in the smooth muscle. In fact, the contractile activity and $[Ca^{2+}]_i$ oscillation of the entire cell cluster were blocked with nifedipine.

Recent studies have shown that ICC play the role of pacemaker cells. They generate electrical activity, i.e., slow waves, which is propagated to smooth muscle cells and produces spontaneous contractions of the muscle layer. One of the characteristic features of the slow wave is dihydropyridine (nifedipine)-resistant activity (5, 11). Nifedipine does not prevent slow wave generation. This indicates that, beside smooth muscle cells, special pacemaker cells are present and that ion channels different from L-type Ca^{2+} channels play a critical role in the pacemaking. The Ca^{2+} imaging with nifedipine combined with subsequent immunohistochemistry showed that $[Ca^{2+}]_i$ oscillation occurs in c-Kit-positive ICC in the cultured cell cluster (Fig. 3). Furthermore, simultaneous recording of $[Ca^{2+}]_i$ and electrical activity in ICC revealed that $[Ca^{2+}]_i$ oscillation in ICC is synchronised with slow waves, and the two are likely to be causally related (Fig. 4). The slow waves seen in the isolated cell cluster are also similar to those observed in intact tissues in their frequency of oscillation (11, 13, 14) and temperature-dependency (our unpublished data). Therefore, the present preparation is a suitable model system for the analysis of the pacemaker mechanism as a minimum unit of the GI muscle layer.

Studies on electrical rhythmicity in ICC have suggested that IP3 receptor-dependent calcium release from ER is crucial for the generation of slow waves. The circular smooth muscle isolated from mutant mice lacking IP3 type 1 receptor failed to generate slow waves, even though the action potential of the smooth muscle was not affected (12, 24). Another group reported that inhibitors of IP3 receptor-dependent release of Ca^{2+} from ER blocked pacemaker activity: a membrane-permeable blocker of IP3 receptor (xestospongin C), and injection of heparin inhibited pacemaker current and slow waves (25). Thus, Ca^{2+} release from ER though IP3 receptor is necessary for $[Ca^{2+}]_i$ oscillation in ICC. It is also well known that ICC have many mitochondria, and that mitochondrial Ca^{2+} uptake is though to be required for electrical pacemaking in ICC. Pacemaker currents were closely related to mitochondrial Ca^{2+} transient: mitochondrial uncouplers (FCCP and CCCP) and respiratory chain inhibitors (antimycin) blocked pacemaker current (25). This is consistent with a previous report that pacemaking in ICC is dependent upon metabolic activity (26, 27). All together, these data suggest that an intracellular calcium event depending upon the periodic release of Ca^{2+} from ER through IP3 receptor and subsequent uptaking of Ca^{2+} by mitochondria is necessary for $[Ca^{2+}]_i$ oscillation in ICC. Although these two events appear to be primary factors in $[Ca^{2+}]_i$ oscillation in ICC, the mechanisms integrating Ca^{2+} handling of ER and mitochondria in ICC and the generation of pacemaker current in the plasma membrane remain to be clarified.

In addition to the intracellular calcium events, the present study of $[Ca^{2+}]_i$ oscillation in ICC demonstrated that the pacemaking mechanism in ICC requires extracellular Ca^{2+} because Ca^{2+} -free bath solution and Mn^{2+} inhibited $[Ca^{2+}]_i$ oscillation in ICC (Fig. 5). The insensitivity to nifedipine clearly shows that Ca^{2+} influx is not mediated by an L-type calcium channel, which is ordinarily required for the contractions of smooth muscle cells. Instead, the channel is thought to be a non-selective cation channel because La^{3+} and Cd^{2+} quickly reduced the amplitude of $[Ca^{2+}]_i$ oscillation and eventually blocked it. On the other hand, the T-type calcium channel is not

likely to contribute to the influx because a considerable amount of Ni^{2+} did not affect $[Ca^{2+}]_i$ oscillation (Fig. 5) (28).

A gene family of TRP channels was cloned recently, and their products are considered to be non-selective cation channels (29-32). Some of them (including TRP4) were reported to be store-operated channels (20, 33). The expression of *trp* genes in the murine and canine GI muscle layers was recently reported. Only full length of *trp4, trp6* and some splice variants were detected in the muscle layer of the mouse GI tract (18). Epperson et al. (2000) reported that freshly isolated or cultured ICC also express only *trp4* and *trp6* (34). These reports suggest that TRP4 and /or TRP6 may be involved in $[Ca^{2+}]_i$ oscillation in ICC. In the present study we showed that $[Ca^{2+}]_i$ oscillation in ICC was blocked by SK&F 96365, which was used as an inhibitor of TRP4 expressed on *Xenopus* oocytes (35). Moreover, thapsigargin that blocks ER Ca^{2+} -ATPases increased and then decreased $[Ca^{2+}]_i$ in ICC, and eventually blocked the oscillations. This indicates that the channel involved in the oscillation was store-operated and activated by the depletion of Ca^{2+} in ER. The sensitivity to store depletion is higher in TRP4 than in TRP6 (29). These data strongly suggested that the non-selective cation channel involved in $[Ca^{2+}]_i$ oscillation in ICC was TRP4. Although it was confirmed that both TRP4 and TRP6 were expressed in the muscle layer of the mouse small intestine by western blotting (Fig. 7), TRP6 was demonstrated intensely in the smooth muscle but not in ICC by immunohistochemistry (data not shown). We thus think that TRP4 is predominant in ICC, whereas TRP6 is a principal type in smooth muscle. The periodic Ca^{2+} release through IP3 receptor may cause depletion of the Ca^{2+} store, which then activates TRP4 spontaneously. This Ca^{2+} influx, mediated by TRP4, might provide pacemaker current in ICC.

By immunohistochemistry TRP4 was located mostly in caveolae shown by colocalization with caveolin-1 labelling. The caveolar distribution of TRP4 was corroborated with immunoelectron microscopy. Caveolae are enriched with many signalling molecules and are abundant in ICC (36, 37). G protein-coupled receptors and receptor tyrosine kinases, concentrated in caveolae, are known to regulate TRP activity

(38, 39). Therefore, it is strongly suggested that neurotransmitters and hormones work on caveolae to modulate the pacemaking function in ICC. Moreover, a recent paper reported the possibility that TRP3 in caveolae formed direct physical interaction with IP3 receptor in ER and mediated Ca^{2+} influx in HEK-293 cells (40). Further studies are necessary to determine the functional relationship between TRP4, caveolae, and IP3 receptor and to understand the mechanism by which pacemaker currents are generated.

In summary, the $[Ca^{2+}]_i$ oscillation we demonstrated in ICC using isolated cell clusters from the mouse small intestine was closely linked to the pacemaker activity. Ca^{2+} influx was necessary for $[Ca^{2+}]_i$ oscillation, and the non-selective cation channel TRP4, located mainly in caveolae, was inferred to mediate the Ca^{2+} entry in ICC.

Acknowledgements

The work was supported by Ministry of Education, Science, Sports, and Culture of Japan and The Japan Clinical Study Group of Esophago-cardiac Region. Thanks are due to Dr. Nishi (Univ. Kumamoto) for antibody ACK2 and to Dr. Satoh (Iwate Medical University) for technical advice on calcium imaging. We also thank Drs. Sanders, Horowitz, Ward and Koh for valuable discussions (Univ. Nevada Reno).

Abbreviations : ICC, interstitial cells of Cajal; $[Ca^{2+}]_i$, intracellular Ca^{2+} concentration; FITC, fluorescein isothiocyanate; TTX, tetrodotoxin; TRP, transient receptor potential; ER, endoplasmic reticulum; IP3, inositol trisphosphate; GI muscle; gastrointestinal muscle.

1 Thuneberg, L. (1982) *Adv Anat Embryol Cell Biol* 71, 1-130.

2 Rumessen, J.J., Mikkelsen, H.B. and Thuneberg, L. (1992) *Gastroenterology* 102, 56-68.

3 Szurszewsky J.H. (1987) :*Electrical basis for gastrointestinal motility*:*Handbook of the gastointestinal tract* 2nd ed., Raven Press, New York.

4 Sanders, K.M. (1996) *Gastroenterology* 111, 492-515.

5 Horowitz, B., Ward, S.M. and Sanders, K.M. (1999) *Annu Rev Physiol* 61, 19-43.

6 Ward, S.M., Burns, A.J., Torihashi, S. and Sanders, K.M. (1994) *J Physiol (Lond)* 480, 91-97.

7 Torihashi, S., Ward, S.M., Nishikawa, S.-I., Nishi, K., Kobayashi, S. and Sanders, K.M. (1995) *Cell Tissue Res* 280, 97-111.

8 Huizinga, J.D., Thuneberg, L., Klüppel, M., Malysz, J., Mikkelsen, H.B. and Bernstein, A. (1995) *Nature* 373, 347-349.

9 Thomsen, L., Robinson, T.L., Lee, J.C.F., Farraway, L.A., Hughes, M.J.G., Andrews, D.W. and Huizinga, J.D. (1998) *Nat Med* 4, 848-851.

10 Koh, S.D., Sanders, K.M. and Ward, S.M. (1998) *J Physiol (Lond)* 513, 203-213.

11 Lee, J.C.F., Thuneberg, L., Berezin, I. and Huizinga, J.D. (1999) *Am J Physiol* 277, G409-G423.

12 Suzuki, H., Takano, H., Yamamoto, Y., Komuro, T., Saito, M., Kato, K. and Mikoshiba, K. (2000) *J Physiol (Lond)* 525, 105-111.

13 Ward, S.M., Ördög, T., Koh, S.D., Baker, S.A., Jun, J.Y., Amberg, G., Monaghan, K. and Sanders, K.M. (2000) *J Physiol (Lond)* 525, 355-363.

14 Malysz,J, Donnelly,G and Huizinga,JD. (2001) *Am J Physiol* 280, G439-G456.

15 Yamazawa, T. and Iino, M. (2002) *J Physiol (Lond)* 538, 823-835.

16 Tokutomi, N., Maeda, H., Tokutomi, Y., Sato, D., Sugita, M., Nishikawa, S., Nishikawa, S., Nakao, J., Imamura, T. and Nishi, K. (1995) *Pflugers Arch* 431, 169-177.

17 Fujita, A. (2001) *Am J Physiol, Cell Physiol* 281, C1727-C1733.

18 Walker, R.L., Hume, J.R. and Horowitz, B. (2001) *Am J Physiol* 280, C1184-C1192.

19 Torihashi, S., Fujimoto, T. and Nakayama, S. (2001) *Neurogastroenterol Motil* 13, 437-437.

20 Philipp, S. Trost, CT., Warnat,J., Rautmann,J., Himmerkus, N., Schroth,G., Kretz, O., Nastainczyk, W., Cavalié, A., Hoth,M. and Flokerzi, V. (2000) *J Biol Chem* 275, 23965-23972.

21 Tokuyasu, K.T. (1989) *J Cell Biol* 108, 43-53.

22 Griffiths, G., Simons, K., Warren, G. and Tokuyasu, T.K. (1986) *Methods Enzymol* 96, 466-483.

23 Stevens,RJ, Publicover,NG and Smith,TK. (2000) *Gastroenterology* 118, 892-904.

24 Suzuki, H. (2000) *Jpn J Physiol* 50, 289-301.

25 Ward, S., Ördög,T, Koh,SD, AbuBaker,S, Jun,JY, Amberg,G, Monaghan,K and Sanders,KM. (2000) *J Physiol (Lond)* 525, 355-363.

26 Nakayama, S., Chihara, S., Clark, J.F., Huang, S.-M., Horiuchi, T. and Tomita, T. (1997) *J Physiol (Lond)* 505, 229-240

27 Huang, S. (1999) *Am J Physiol* 276, G518-G528.

28 Farrugia, G. (1999) *Annu Rev Physiol* 61, 45-84.

29 Birnbaumer, L., Zhu, X., Jiang, M., Boulay, G., Peyton, M., Vannier, B., Brown, D., Platano, D., Sadeghi, H., Stefani, E. and Birnbaumer, M. (1996) *Proc Natl Acad Sci U S A* 93, 15195-15202.

30 Harteneck, C., Plant, T.D. and Schultz, G. (2000) *Trends Neurosci* 23, 159-166.

31 McKay, R.R., Szymeczek-Seay, C.L., Lievremont, J.-P., Bird, G.S.J. and Zitt, C. (2000) *Biochem J* 351, 735-746.

32 Clapham, D.E., Runnels, L.W. and Strubing, C. (2001) *Nautre reviews neuroscience* 2, 387-396.

33 Freicher,M, Suh,SH, Pfeifer,A, Schweig,U, Trost,C, Weissgerber,P, Biel,M, Philipp,S, Freise,D, Droogmans,G., Hofmannn,F., Flockerzi, V. and Nilius, B. (2001) *NatCell Biol* 3, 121-127.

34 Epperson,A, Hatton,WJ, Callaghan,B, Doherty,P, Walker,RL, Sanders,KM, Ward,SM and Horowitz,B. (2000) *Am J Physiol* 279, C529.

35 Kinoshita, M., Akaike, A., Satoh, M. and Kaneko, S. (2000) *Cell Calcium* 28, 151-159.

36 Rumessen, J.J. (1994) *Dan Med Bull* 41, 275-293.

37 Okamoto, T., Schlegel, A., Scherer, P.E. and Lisanti, M.P. (1998) *J Biol Chem* 273, 5419-5422.

38 Boulay, G., Zhu, X., Peyton, M., Jiang, M., Hurst, R., Stefani, E. and Birnbaumer, L. (1997) *J Biol Chem* 272, 29672-29680.

39 Tang, Y., Tang, J., Chen, Z., Trost, C., Trost, V., Li, M., Ramesh, V. and Zhu, X.M. and Flockerzi, V. (2000) *J Biol Chem* 275, 37559-37564.

40 Lockwich, T., Singh, B.B., Liu, X. and Ambudkar, I.S. (2001) *J Cell Biol* 276,42401-42408.

Figure legends

Figure 1. Phase-contrast microscopy and immunohistochemistry of a cell cluster isolated from the mouse small intestine and cultured for 2 days. (A) Phase-contrast image shows a round cell cluster about 100 μm in diameter. Bar = 50 μm applied to A-C. (B) Immunohistochemistry for γ-enteric actin on the same cell cluster shown in A indicates that most cells are smooth muscle cells. (C) Immunohistochemistry for c-Kit identifies ICC in the same cluster in panels A, B. ICC are located randomly in the cluster. (D) Immunohistochemistry for PGP9.5 shows enteric neurons. Large clusters, i.e., more than 100 μm in diameter, sometimes contain enteric neurons. Bar = 50 μm.

Figure 2. $[Ca^{2+}]_i$ oscillations in a cultured cell cluster. The cluster was loaded with 10 μM of fluo4 AM ester and the temporal change of the fluorescent intensity was measured. (A) The minimum level of $[Ca^{2+}]_i$ in control solution (at 35 °C) is shown in a pseudocolour ratioed image. (B) The maximum level of $[Ca^{2+}]_i$ is shown in pseudocolour ratioed image. Note that the size of the cluster in A is smaller than that in B, indicating contraction of the cluster. Bar = 50μm (C) Corresponding time courses of $[Ca^{2+}]_i$ in the cluster. Green, red and black lines show oscillations observed at three points indicated by respective colours in panels A and B. All points demonstrate clear and synchronised $[Ca^{2+}]_i$ oscillations. The frequency was 20.4 cycles/min.

Figure. 3. $[Ca^{2+}]_i$ oscillation in a cell cluster in the presence of 1 μM nifedipine. (A) A pseudocolour ratioed image showing the minimum level of $[Ca^{2+}]_i$. (B) A ratioed image showing the maximum level of $[Ca^{2+}]_i$. . $[Ca^{2+}]_i$ rises only in limited areas, but not as a whole. (C) A phase contrast micrograph of the same cell cluster shown in A and B. (D) Immunohistochemistry for c-Kit shows localisation of ICC in the same cluster. Points (1)-(3) are respective to those in A and B. Note that points (1) and (2) correspond to c-Kit-positive ICC, whereas point (3) is in a c-Kit-negative area. Points (1) and (2) showed a significant increase of $[Ca^{2+}]_i$, but point (3) did not. Bar = 20 μm applied to A-D. (E)

Corresponding time courses of $[Ca^{2+}]_i$ in the cluster. Green, red and black lines show the movement obtained from the three points indicated by respective colours in A and B. Point (1) in black and point (2) in red clearly show $[Ca^{2+}]_i$ oscillations at 19.2 cycles/min in frequency. Point (3) in green does not show such an oscillation.

Figure 4. Simultaneous recordings of the electrical activity and $[Ca^{2+}]_i$ in ICC. Upper panel shows electrical activity and the lower panel indicates $[Ca^{2+}]_i$ movements in ICC (thick line) and non-ICC region (thin line) in the presence of 1 μM nifedipine. Electrical activities corresponding to slow waves were synchronised with $[Ca^{2+}]_i$ oscillations in ICC. The frequency was 18.3 cycles/min. Depolarisation (0.16 mV) are temporally associated with increases of $[Ca^{2+}]_i$ in ICC and these two show tight temporal relationship.

Figure 5. Effects of Ca^{2+} -free condition and various cations on $[Ca^{2+}]_i$ oscillations in ICC (thick lines) and non-ICC cells (thin lines) in the presence of 1 μM nifedipine. (A) In Ca^{2+} -free solution, $[Ca^{2+}]_i$ oscillations in ICC was abolished within 1 min. (B) Quenching by Mn^{2+} quickly diminished $[Ca^{2+}]_i$ oscillations in ICC. (C) La^{3+} blocked $[Ca^{2+}]_i$ oscillations in ICC. (D) Cd^{2+} increased the intensity of fluorescence and disturbed the oscillation. (E) Ni^{2+} (50 μM), a T-type channel blocker, did not affect the oscillation in ICC.

Figure 6. Effects of SK&F96365 and thapsigargin on $[Ca^{2+}]_i$ oscillation in ICC in the presence of 1 μM nifedipine. (A) SK&F96365 abolished $[Ca^{2+}]_i$ oscillations in ICC. (B) Thapsigargin, a blocker of Ca^{2+} pump in ER, hampered $[Ca^{2+}]_i$ oscillations in ICC. It increased and then decreased Ca^{2+} level and inhibited the oscillation eventually.

Figure 7. Immunohistochemistry and western blotting of TRP. (A-D) Whole mount preparation of the muscle layer. Bar = 10μm (A) Anti-c-Kit antibody shows distribution of ICC at the level of the myenteric plexus. They are multipolar cells connected with each other forming a network. (B) Immunolabeling of TRP4. (C) Merged image of A and B

shows colocalization of c-Kit and TRP4 in ICC. Some-non-ICC cells expresses TRP4, but the expression of TRP4 is stronger in ICC than non-ICC cells. (D) A control processed without primary antibodies does not show any immunoreactivity. (E) Western blotting analysis proved that both TRP4 and TRP6 are expressed in the muscle layer. Lanes 1, 3 and 5 are probed by two different anti-TRP4 antibodies (a product of Alomone labs, and Ab236) and anti-TRP6 antibody, respectively. Lanes 2, 4 and 6 were treated with absorbed antibodies (pre-incubated with 10-fold excess of the antigens) used in lanes 1, 3, and 5, respectively. Ab236 recognised an additional band below 66K, which was also absorbed in the control.

Figure 8. Distribution of TRP4 in ICC. (A-C) Double immunolabeling of TRP4 and caveolin-1in ICC. Bar = 10 μm. TRP4 (A) and caveolin-1 (B) were both densely distributed along the cell edge (arrowheads). (C) Merged image of A and B. (D) A control processed without primary antibodies does not show any immunoreactivity.

Figure 9. Immunoelectron microscopy of TRP4 in ICC, which is caveolae-rich cell located between the circular and longitudinal muscle layers where ICC are densely distributed. The cell has neither myofilaments nor dense bodies. TRP4 immunoreactivity marked by colloidal gold particles are located in caveolae. Asterisks indicate the lumen of caveolae, which were cross-sectioned and thus appeared as vesicles. Control sections processed without primary antibody did not show any specific immunoreactivity (data not shown). Bar = 100 nm.

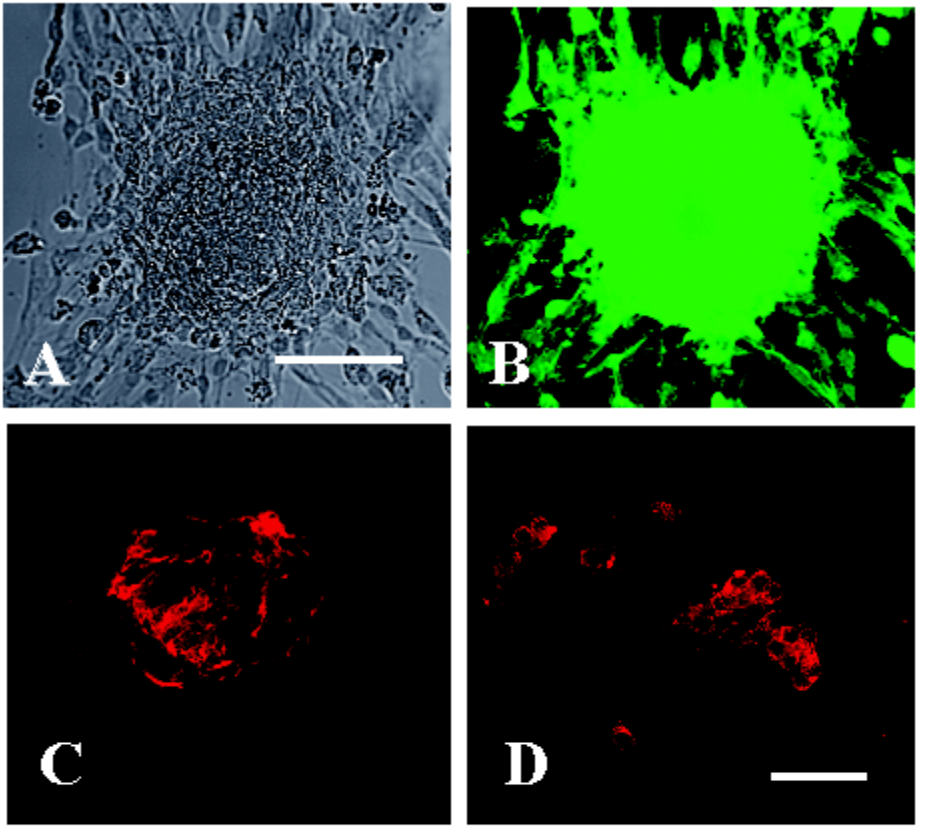

Fig. 1 *Torihashi et al.*

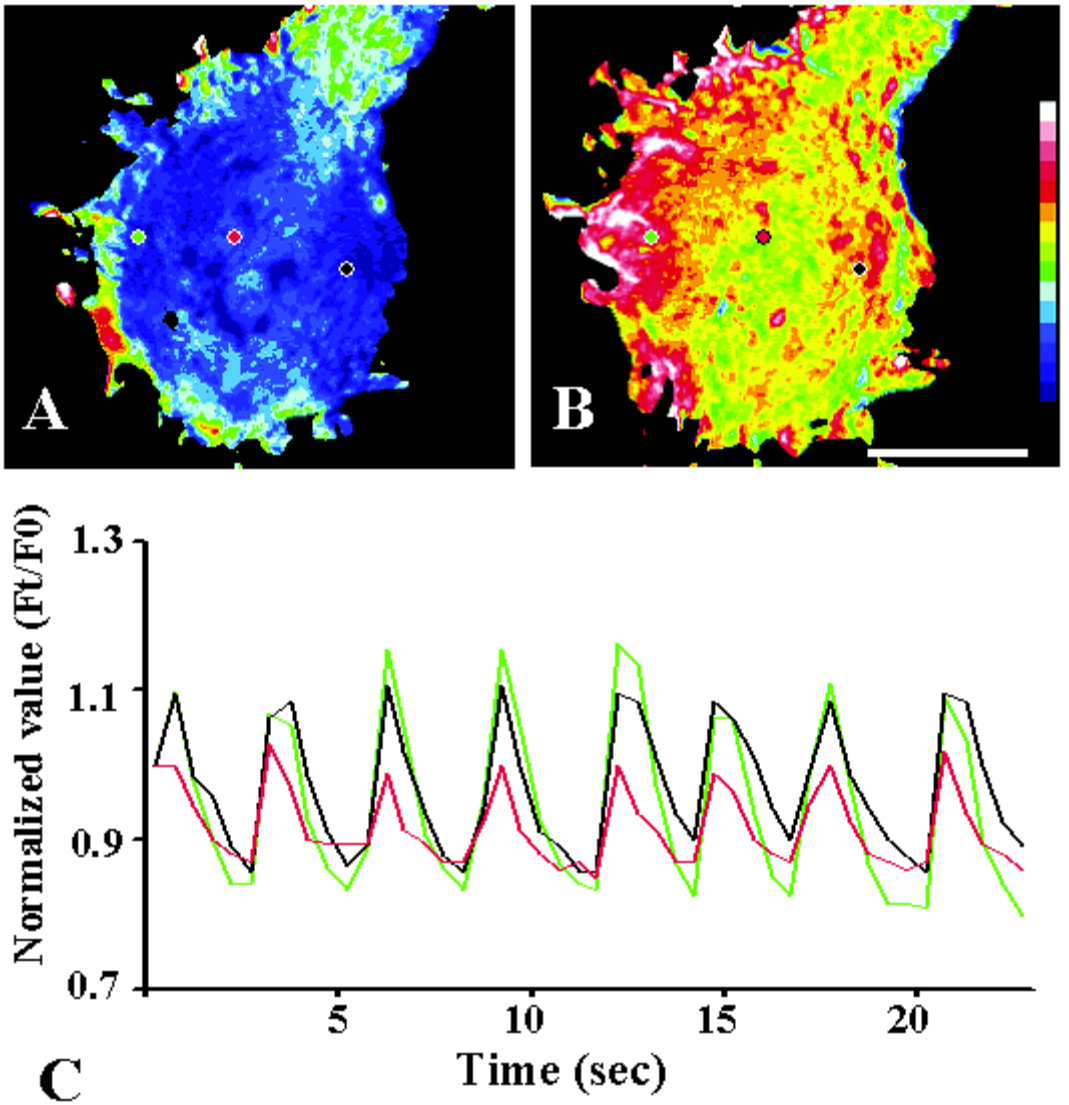

Fig. 2 ***Torihashi et al.***

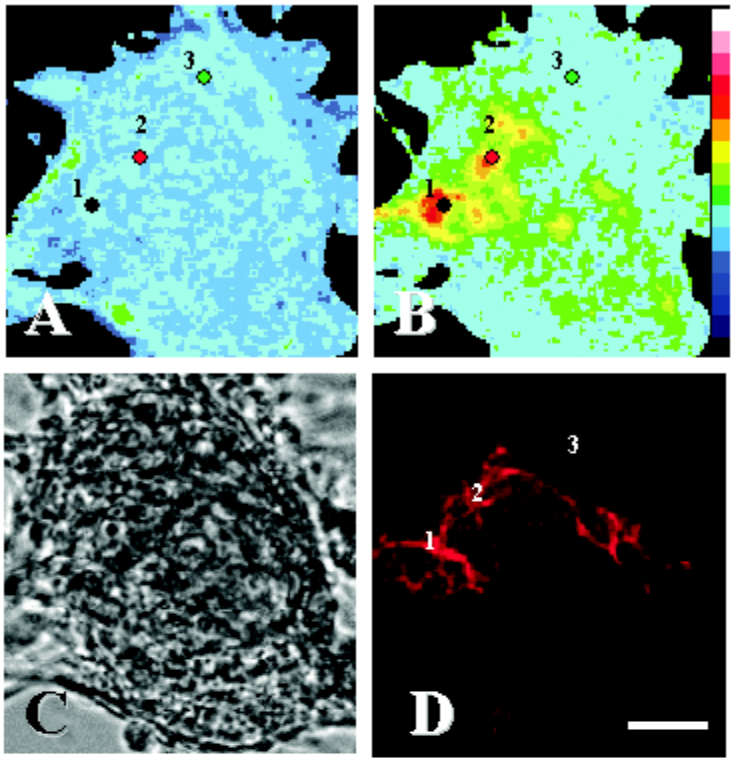

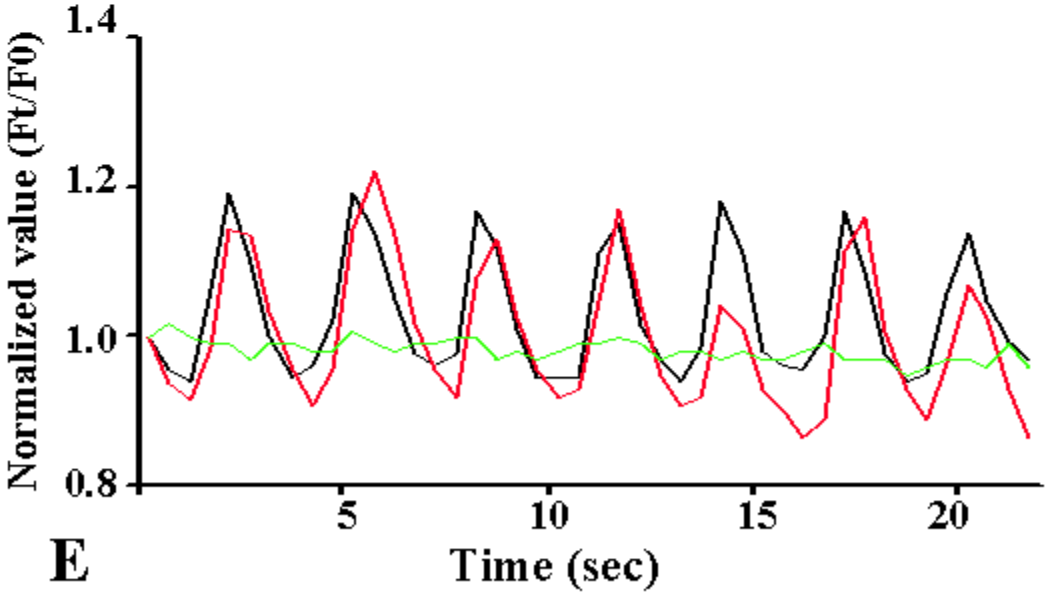

Fig. 3 ***Torihashi et al.***

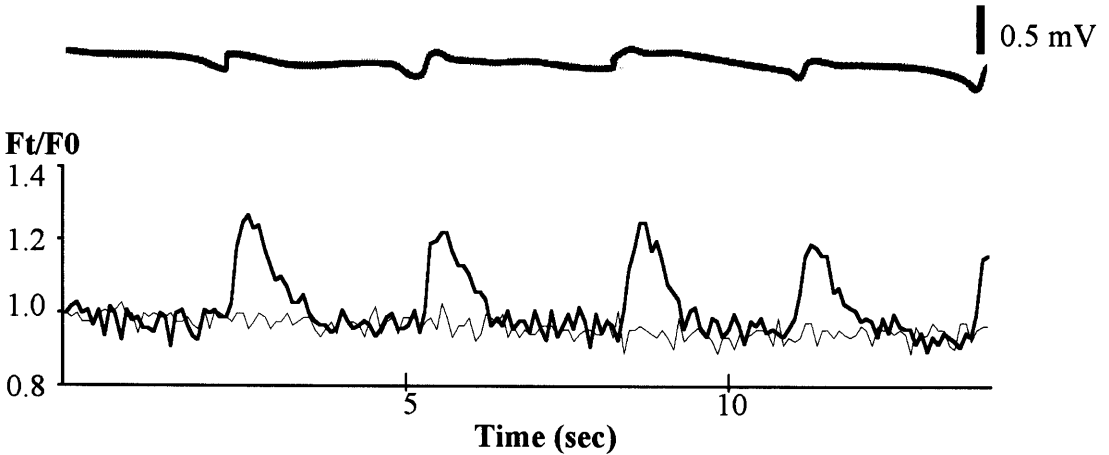

Fig. 4 ***Torihashi et al.***

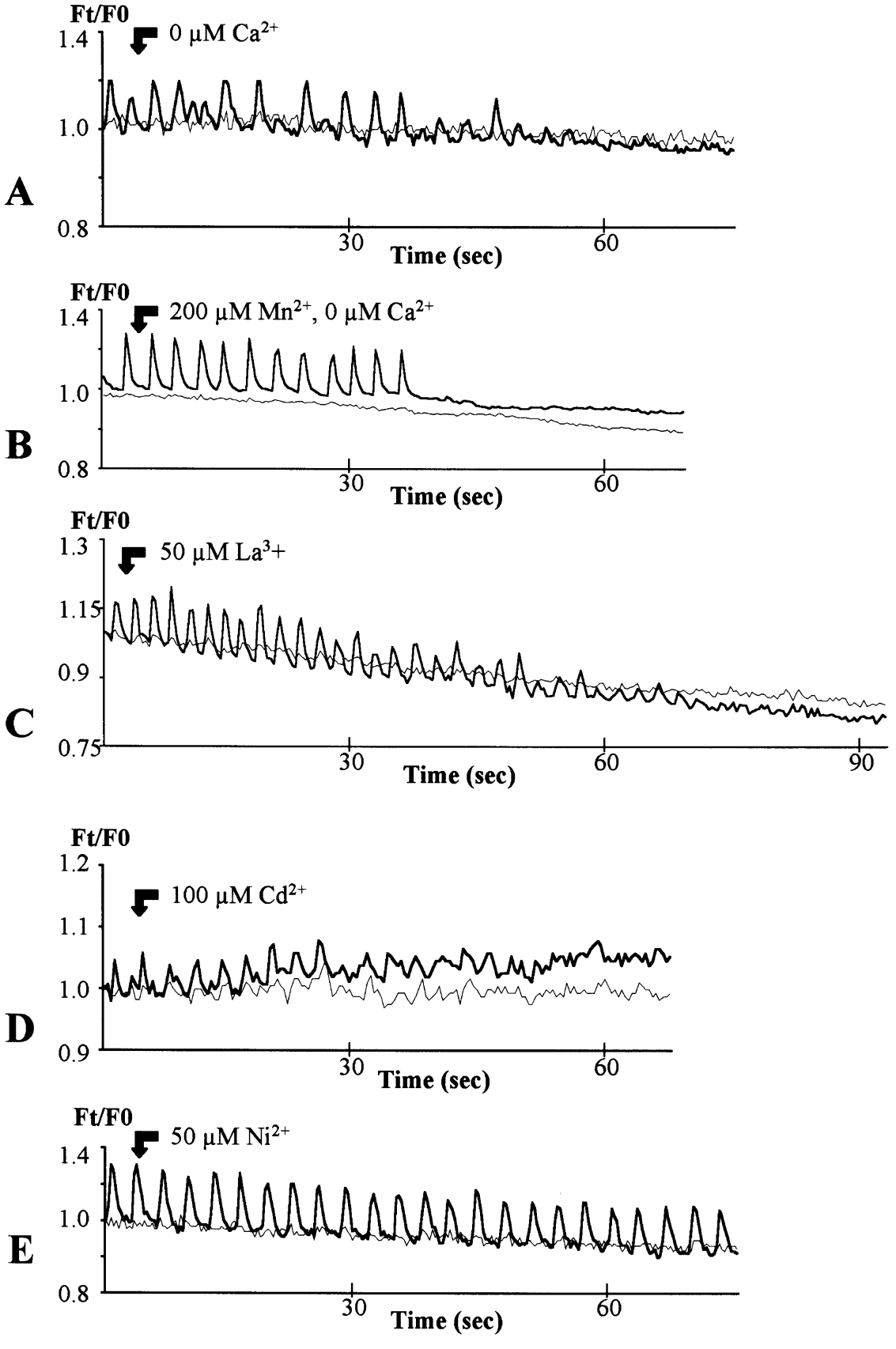

Fig. 5 ***Torihashi et al.***

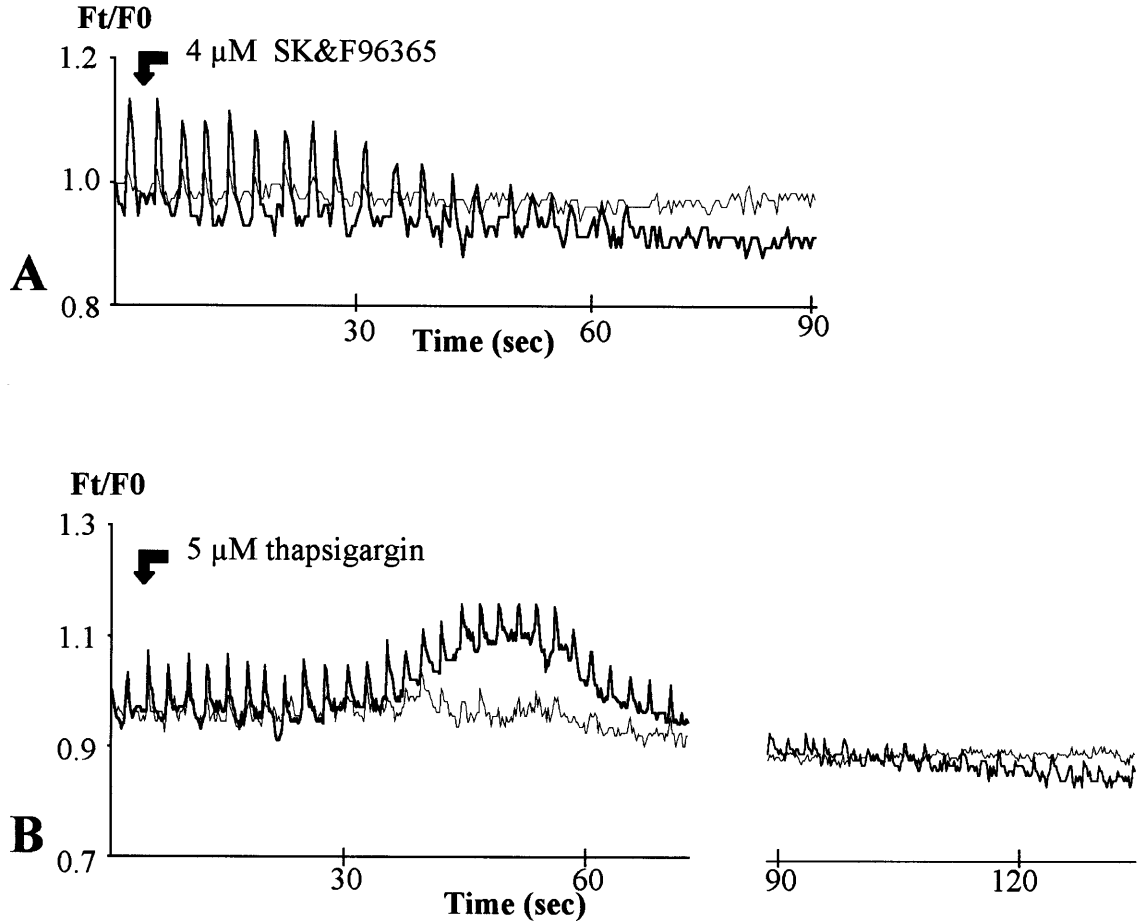

Fig. 6 ***Torihashi et al.***

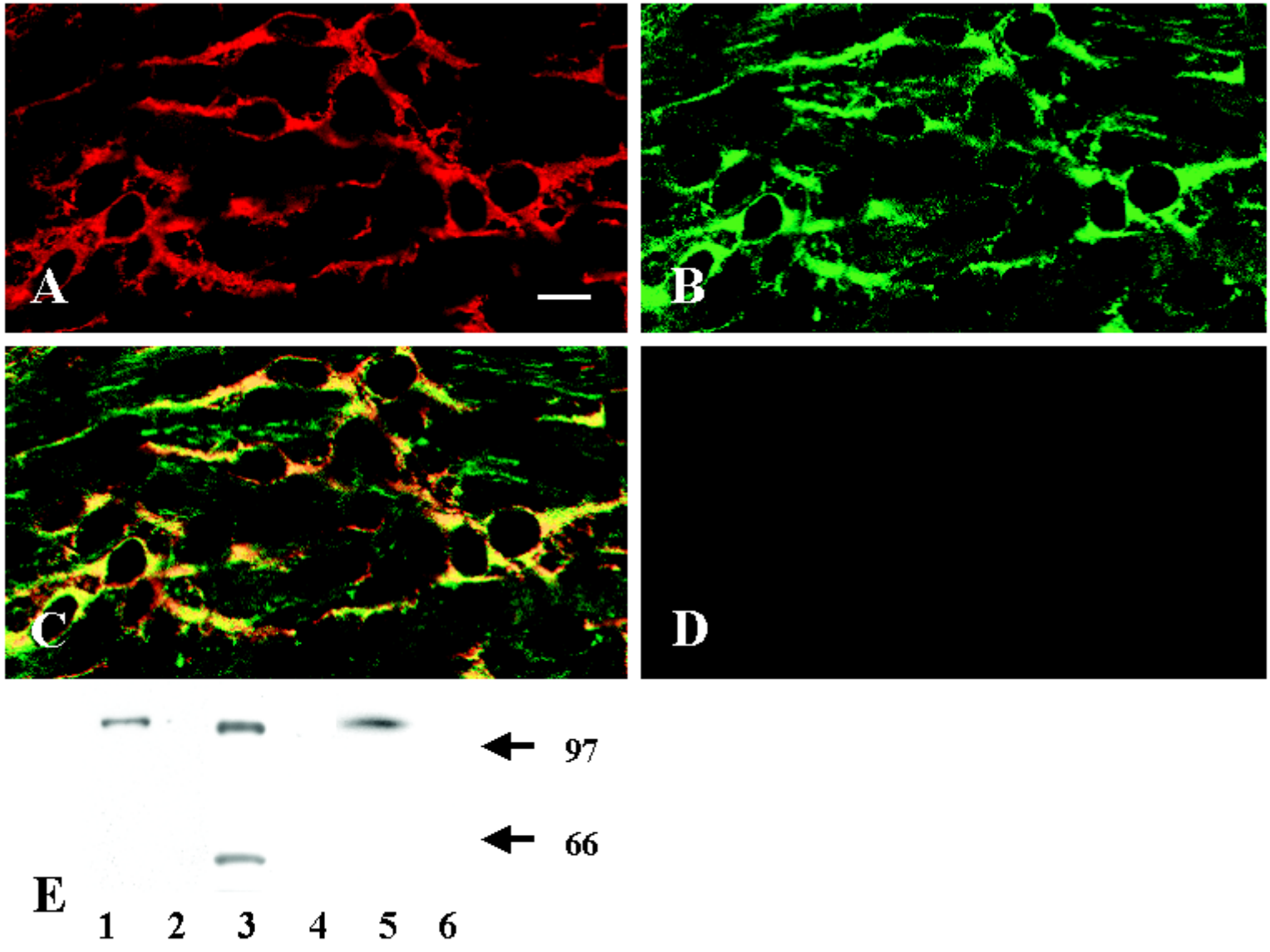

Fig. 7 *Torihashi et al.*

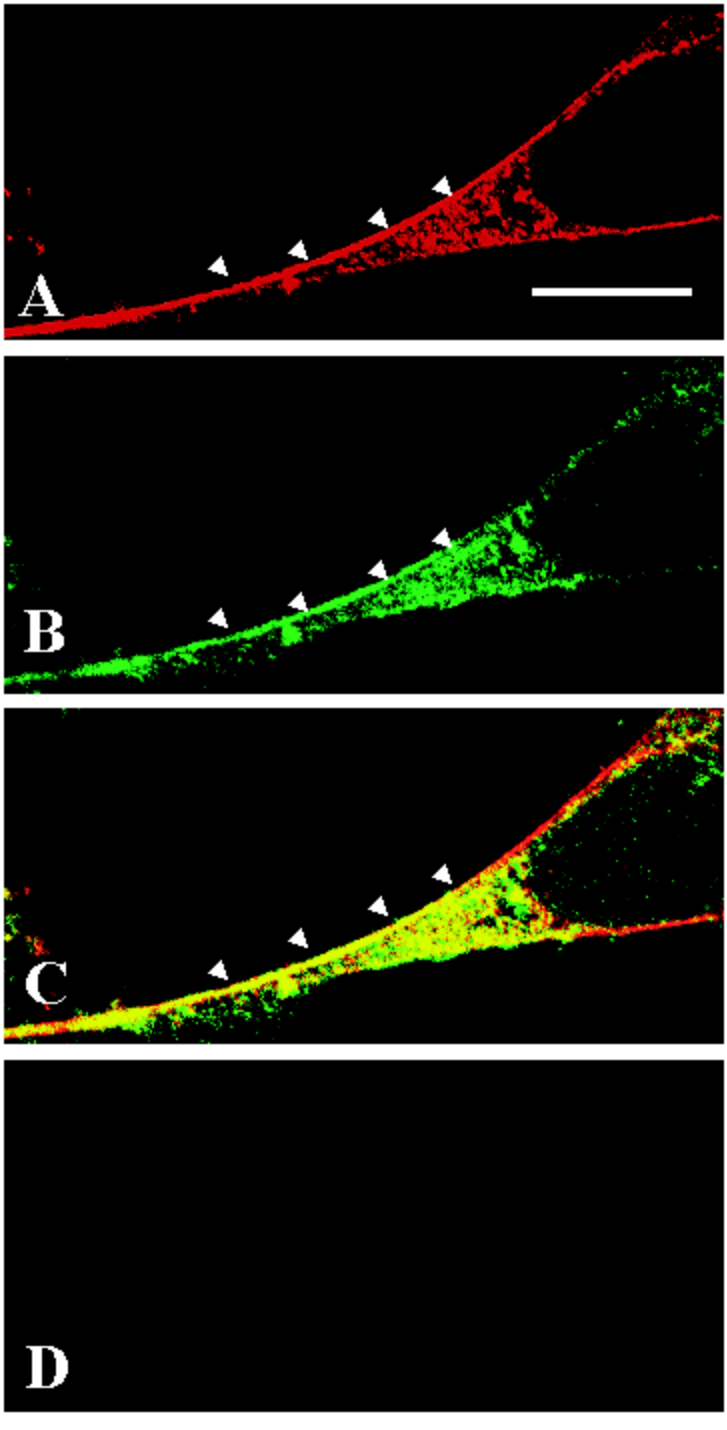

Fig. 8 *Torihashi et al.*

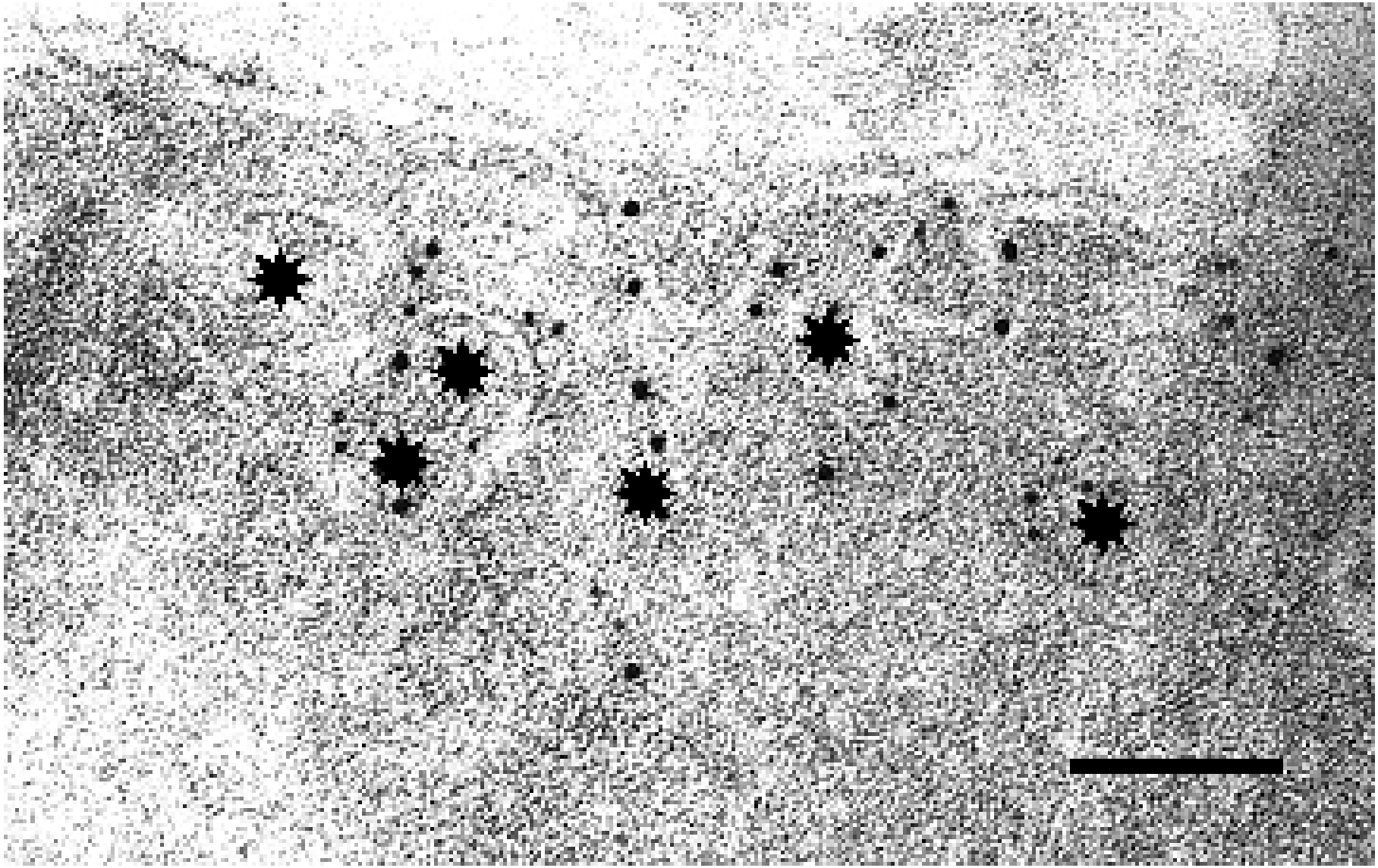

Fig. 9 *Torihashi et al.*